IFSCC 2025 full paper (IFSCC2025-1197)

"Effects of CP-AcT on Melanin Synthesis and Regulation of Inflammatory Factors"

Minhua Hong [1], Xianglong Zhao [1], Jin Liu [1], Diqing Wang [1], Hui Wang [1] and Rong Tang [1]

[1] Shanghai Peptide Biotechnology Co., Ltd, Shanghai, China

1. Introduction

Melanin, a crucial pigment component synthesized and stored in melanosomes within melanocytes [1,2], serves as the foundation for conferring unique skin, hair, and iris colors in humans [1]. It also plays an indispensable physiological barrier role in maintaining skin health and protecting against external environmental stressors such as ultraviolet radiation [3,4]. The biosynthetic pathway of melanin is regulated by the tyrosinase family (TYR, TYRP1, TYRP2), which transforms tyrosine into melanin precursors through a series of enzymatic cascade reactions [1]. This process involves intricate cross-regulation by multiple signaling pathways, including cAMP/PKA, MAPK/ERK, and Wnt/β-catenin pathways [5-7]. Recent studies have further revealed that MITF, as a core transcription factor, integrates upstream signaling inputs to directly regulate the expression of the tyrosinase family [8,9].

Abnormal melanin production is closely linked to various diseases. For instance, vitiligo is associated with autoimmune destruction of melanocytes, involving abnormal activation of the STAT1-IRF1 pathway [10,11]. Conversely, the depletion of neuromelanin in the substantia nigra pars compacta in Parkinson's disease shows a significant positive correlation with the degeneration of dopaminergic neurons [12-14]. Existing therapies such as narrowband UVB phototherapy and topical glucocorticoids exhibit certain efficacies but suffer from high recurrence rates (>60%) and long-term safety concerns. Therefore, there is an urgent need to develop natural melanogenic agents that target melanin synthesis pathways and possess anti-inflammatory properties.

In this study, we systematically evaluated the mechanism of action of CP-AcT, a compound formulation comprising palmitoyl tripeptide-1 GHK-Cu (pal-GHK-Cu) and N-acetyl-L-tyrosine, using the Luminex 200 liquid suspension chip system combined with protein chip technology. Palmitoyl copper peptide stabilizes the active center of tyrosinase through Cu^{2+}, while N-acetyl-L-tyrosine, as a preferred substrate for TYR, reduces the Km value of the enzymatic reaction. The synergistic effects of these two components potentially optimize melanin synthesis efficiency through dual regulation of gene expression and enzymatic kinetic parameters while modulating the inflammatory microenvironment, offering a novel strategy for the treatment of pigmentary disorders.

2. Materials and Methods

2.1 Determination of the Effect of CP-AcT on A375 Cell Viability

The effect of CP-AcT on A375 cell viability was assessed using the MTT assay to determine the subsequent experimental concentrations.

(1) Cells in the logarithmic growth phase were harvested, digested with trypsin to obtain a cell suspension, and the cell density was adjusted to 2×10^4 cells/mL using complete DMEM culture medium. The cells were then uniformly seeded into a 96-well plate and incubated overnight.
(2) The original culture medium was aspirated and replaced with fresh medium containing CP-AcT at various concentrations. Five replicate wells were established for each concentration, and the cells were continuously cultured for 48 h.
(3) The drug-containing medium was aspirated, and the wells were rinsed once with PBS. MTT solution (5 mg/mL) prepared in DMEM medium was rapidly added to each well. To prevent cell desiccation and death, the MTT addition was performed in cycles of six wells per batch. The cells were further incubated for 4 h.
(4) The MTT solution within the wells was aspirated, and 150 μL of DMSO was added. The plate was vigorously shaken at 600 rpm for 5 min to fully dissolve the formazan crystals. Subsequently, the absorbance was measured using a microplate reader at a test wavelength of 570 nm and a reference wavelength of 630 nm to determine cell viability.The formula for calculating cell viability is as follows:

Relative cell viability (%) = OD_((570-630) sample) / OD_((570-630) control) × 100

2.2 Effect of CP-AcT on Melanin Content in A375 Cells

(1) Cells in the logarithmic growth phase were harvested, digested with trypsin to obtain a cell suspension, and the cell density was adjusted to 8×10^4 cells/mL using complete DMEM culture medium. The cells were uniformly seeded into a 6-well plate and incubated overnight. This experimental design includes three groups: a positive control group (treated with α-MSH), an experimental group (treated with CP-AcT), and a negative control group (without drug treatment).
(2) The original culture medium was aspirated and replaced with fresh medium containing the test compound. The cells were then cultured in a 37℃, 5% CO_2 incubator for 48 h.
(3) The supernatant was aspirated, and the wells were rinsed twice with PBS. The cells were subsequently digested with trypsin, and the digestion was terminated using culture medium. The cell suspension was collected into centrifuge tubes and centrifuged at 12,000 rpm for 10 min at 4℃.
(4) The supernatant was discarded, and 1 mol/L NaOH solution containing 10% DMSO was added to each tube. The samples were heated in a 100℃ metal bath for 1 h until the cell pellets were completely dissolved. Following dissolution, the samples were centrifuged again at 12,000 rpm for 10 min at 4℃.
(5) An 80 μL aliquot of the supernatant was transferred to a 96-well plate, and the absorbance was measured at 405 nm using a microplate reader. The formula for calculating the intracellular relative melanin content is as follows:

Relative melanin content (%) = (A_{405} sample / A_{405} control) × 100

2.3 Effect of CP-AcT on Tyrosinase Activity in A375 Cells

(1) Cells in the logarithmic growth phase were harvested, digested with trypsin to obtain a cell suspension, and the cell density was adjusted to 8×10^4 cells/mL using complete DMEM culture medium. The cells were uniformly seeded into a 6-well culture plate and incubated overnight in a cell culture incubator. This experimental design includes three groups: a positive control group (treated with α-MSH), an experimental group (treated with CP-AcT), and a negative control group (without drug treatment).

(2) The original culture medium was aspirated and replaced with fresh medium containing the test compound. The cells were co-incubated with the test substance and placed back into the incubator for a 48-hour continuous culture.
(3) The culture medium was aspirated, and the wells were rinsed twice with pre-chilled PBS. Western and IP lysis buffer containing 1 mM PMSF was added, followed by incubation on ice for 15 min. The lysate was transferred to pre-chilled Eppendorf (EP) tubes, vortexed for 7 min, and then centrifuged at 10,000 rpm for 10 min at 4℃.
(4) The supernatant was collected, and the protein concentration in the supernatant was determined using a BCA protein assay kit according to the manufacturer's instructions. An aliquot of 100 μg of the supernatant and 50 μL of 1 mg/mL L-DOPA were transferred to a 96-well plate. The mixture was co-incubated at 37℃ for 1 h, rapidly placed into a microplate reader, and the absorbance was measured at 490 nm. The relative tyrosinase activity of the test substances was calculated using the following formula:

$$\text{Relative tyrosinase activity (\%)} = (A_{490}\ \text{sample} / A_{490}\ \text{control}) \times 100.$$

2.4 Quantitative Gene Expression Detection Study
(1) A375 melanoma cells were used. The cell density was adjusted to 6×10^4 cells/mL using complete DMEM medium. Cells were uniformly seeded into a 24-well plate and incubated overnight. This experiment establishes an experimental group (CP-AcT) and a negative control group without drug intervention.
(2) The original medium was aspirated and replaced with fresh medium containing the test compound. The cells were cultured in the incubator for 48 h.
(3) After aspirating the supernatant, lysis mixture was added to lyse the cells. The lysates were stored at −80℃ for long-term preservation.
(4) Cell lysates and lysis mixture were thawed and equilibrated to room temperature. The mixture was incubated at 37℃ for 30 min. The probe set & blocking reagent were thawed and mixed. The probe set was briefly centrifuged to collect the pellet. Proteinase K was stored on ice, and capture beads were kept protected from light. If sample dilution was required, diluted lysis mixture (1 volume of lysis mixture and 2 volumes of nuclease-free water) was used to adjust the sample volume to 80 μL. 20 μL of working bead mix was added to each well of the hybridization plate, followed by 80 μL of cell lysates and diluted lysis mixture. The plate was sealed and incubated at 54 ± 1℃ with shaking at 600 rpm for 18–22 h.
(5) Pre-amplifier solution, amplifier solution, and label probe solution were equilibrated to room temperature and incubated at 37 ℃ for 30 min for activation. SAPE diluent was prepared and stored at room temperature. The hybridization plate was centrifuged and unsealed, and the contents were transferred to a magnetic separation plate. The plate was washed using an automated washer, and residual solution was removed by inversion. Pre-amplifier solution, amplifier solution, and label probe solution were sequentially added to the wells, followed by washing steps. After incubation with SAPE working reagent, the plate was washed again. The SAPE reaction was performed, followed by another wash. 130 μL of SAPE wash buffer was added to each well. The plate was shaken, and fluorescence signals were measured using a microplate reader.

2.5 Protein Microarray Detection Study
(1) Collect the cell supernatants from the quantitative gene detection study after the cells had been cultured with the test substance for 48 h and transfer them into new plates. The supernatants can be stored at -80℃.
(2) Prepare 1× wash buffer (by diluting 10× wash buffer with distilled water at a ratio of 1 : 9). Prepare the cell supernatants, standards, and a blank sample.

(3) Wet the filter plate with 1× Bio-Plex assay buffer. Add 50 μL of 1× beads to each well. Wash the plate twice using 1× wash buffer.
(4) Add samples, standards, a blank, and a control. After a 30-minute incubation, wash the plate. Then, add 1× detection antibodies and continue incubating for another 30 min. Wash the plate again. Finally, add 1× SA-PE, incubate for 10 min, and wash the plate. (For all the above washing steps, use 1× wash buffer and wash three times each time.)
(5) Add 125 μL of Bio-Plex Assay buffer, shake the plate gently, and then proceed with detection and analysis.

2.6 Western Blot Analysis of the Effect of CP-AcT on the Protein Levels Involved in Melanin Synthesis

(1) Take the cells in the logarithmic growth phase, digest them with trypsin to obtain a cell suspension, adjust the cell density to 8×10^4 cells/mL with complete medium, and evenly inoculate the cells in a 6-well plate. Incubate overnight in an incubator.
(2) Aspirate the original medium, add α-MSH and fresh DMEM medium containing the test substance to incubate together with the cells, and continue to culture in the incubator for 48 h;
(3) After incubation for 48 h, the cells were pre-cooled and washed twice with PBS. Strong IP lysis buffer containing 1 mM PMSF was added to each well, and the cells were lysed on ice for 15 min. After thoroughly pipetting the cells, they were transferred to the pre-cooled EP tubes, subjected to vortex oscillation for 7 min at 12,000 rpm/min, 4℃, and centrifuged for 10 min. Collect the supernatant in EP (placed on ice);
(4) Draw the supernatant and use the BCA protein quantification kit to test the protein concentration in the lysis buffer as per the instructions. Calculate the volume of the sample loading buffer required for the lysis supernatant of each test substance.
(5) After mixing with a certain amount of loading buffer according to the calculation results, heat and boil at 100℃ for 5 min, and store at -20℃ for future use.
(6) Protein samples (30 μg) were isolated using 12% concentration SDS-PAGE gel. The protein bands were transferred onto PVDF membranes, sealed with blocking solution at 25℃ for 4 h, and incubated overnight with the primary antibody at 4℃: anti-TYR (1:1000), anti-DCT (1:1000), anti-EDN3 (1:1000), and anti-GAPDH (1:10000). After incubation, washed three times with TBST buffer, then incubated with the secondary antibody at 37℃ for 1 h, washed three times with TBST, developed color with ECL luminescent reagent, and photographed.

3. Results

3.1 The Effect of CP-AcT on Cell Viability

In this study, we first conducted a cytotoxicity assay of the compound CP-AcT on A375 cells to evaluate its safety profile for the cells, as illustrated in Figure 1.
Cell viability was assessed using the MTT assay after treating the cells with different concentrations of CP-AcT for 48 h. The results indicated that CP-AcT had virtually no impact on A375 cell viability at concentrations below 2 μg/mL. In this experiment, α-MSH was employed as a positive control. The MTT assay results demonstrated that α-MSH exhibited no significant cytotoxicity at concentrations below 200 nM.
Therefore, for subsequent experiments, the maximum concentration of CP-AcT tested was set at 2 μg/mL. Meanwhile, α-MSH was used as a positive control at a concentration of 50 nM.

3.2 The Effect of CP-AcT on Melanin Content in Cells

We measured the melanin content in A375 cells after a 48-hour incubation period with CP-AcT. As depicted in Figure 2, both α-MSH and CP-AcT significantly elevated the melanin content within the cells. The impact of CP-AcT on melanogenesis exhibited a dose-dependent

pattern. When compared to the negative control group, the positive control (α-MSH) stimulated melanin production, leading to a 12% increase in melanin content. Notably, cells treated with CP-AcT demonstrated an even more pronounced effect, with melanin content increasing by 17%, which surpassed the elevation observed in the positive control group.

3.3 The Effect of CP-AcT on Tyrosinase Activity

Tyrosinase catalyzes the oxidation of tyrosine to dopa in melanocytes, which is a pivotal step in melanin synthesis. Consequently, we investigated the impact of CP-AcT on tyrosinase activity within A375 cells. L-dopa was utilized as the substrate to measure tyrosinase activity after a 48-hour drug treatment period.

The results, as presented in Figure 3, reveal that when comparing the tyrosinase activity in the CP-AcT-treated group with that of the control group, CP-AcT exhibited a more pronounced stimulatory effect on tyrosinase activity. This indicates that CP-AcT effectively enhances the catalytic function of tyrosinase, thereby potentially accelerating the melanin synthesis pathway in A375 cells.

3.4 The Effect of CP-AcT on Gene Transcription

The transcriptional analysis of 37 genes is illustrated in Figure 4. The results indicate that CP-AcT modulates the transcription levels of key genes associated with melanoma cells, including *PTGS2*, *OCA2*, *SLC45A2*, *TYR*, *DCT*, *EDN3*, *POMC*, and *MET*.

Upon specific analysis of seven genes implicated in melanocyte proliferation, melanin synthesis, or metabolism, we observed that, compared to the negative control group, CP-AcT significantly upregulated the relative transcription levels of *DCT*, *PTGS2*, *SLC45A2*, *EDN3*, and *TYR* ($P < 0.01$), as well as *OCA2* and *MET* ($P < 0.05$). Concurrently, CP-AcT markedly reduced the relative expression level of *IL1A* ($P < 0.01$).

These findings suggest that CP-AcT regulates the transcription levels of various genes in A375 melanoma cells. Specifically, the relative expression levels of *EDN3*, *DCT*, *TYR*, *PTGS2*, *OCA2*, *SLC45A2*, and *MET* increased by 63.28%, 256%, 91.95%, 73.33%, 56.62%, 73.16%, and 18.54%, respectively (as shown in Figure 5).

Moreover, CP-AcT modulated the expression levels of inflammation-related genes. The relative expression level of *IL-1RN* was elevated by 76.08%, while that of *IL-1A* was downregulated by 80.47% (as depicted in Figure 6).

3.5 The Effect of CP-AcT on Inflammatory Cytokines

Following the detection of supernatants from CP-AcT-treated samples using a protein microarray, the research findings, as depicted in Figure 7, reveal that CP-AcT significantly inhibits the relative expression levels of the pro-inflammatory cytokines IL-1α ($P < 0.01$) and IL-6 ($P < 0.05$). Concurrently, CP-AcT markedly promotes the relative expression of the anti-inflammatory cytokines IL-1ra and IL-10, with statistical significance ($P < 0.05$).

3.6 Verification of Protein Expression in the Melanogenesis Pathway via Western Blot

Three relevant proteins influenced by CP-AcT were detected, including two pivotal enzymes directly involved in melanin synthesis, TYR and DCT, as well as EDN3, an upstream protein in the melanogenesis signaling pathway. Western blot analysis was employed to compare the expression levels of these key proteins in melanoma cells treated with different samples.

As illustrated in Figure 6, the positive control (α-MSH) enhanced the expression of TYR and DCT but had no discernible impact on EDN3 expression, which aligns with the established melanin signaling pathway. Notably, treatment of cells with CP-AcT resulted in increased protein expression of TYR, EDN3, and DCT.

These findings suggest that CP-AcT not only promotes the expression of melanin-related proteins TYR and DCT, which are directly implicated in melanin synthesis, but also upregulates the expression of EDN3, an upstream regulator in the melanogenesis signaling cascade. Collectively, these results underscore the role of CP-AcT in modulating the melanogenesis pathway at multiple levels, from upstream signaling to downstream enzymatic activity, thereby potentially influencing melanin production in melanoma cells.

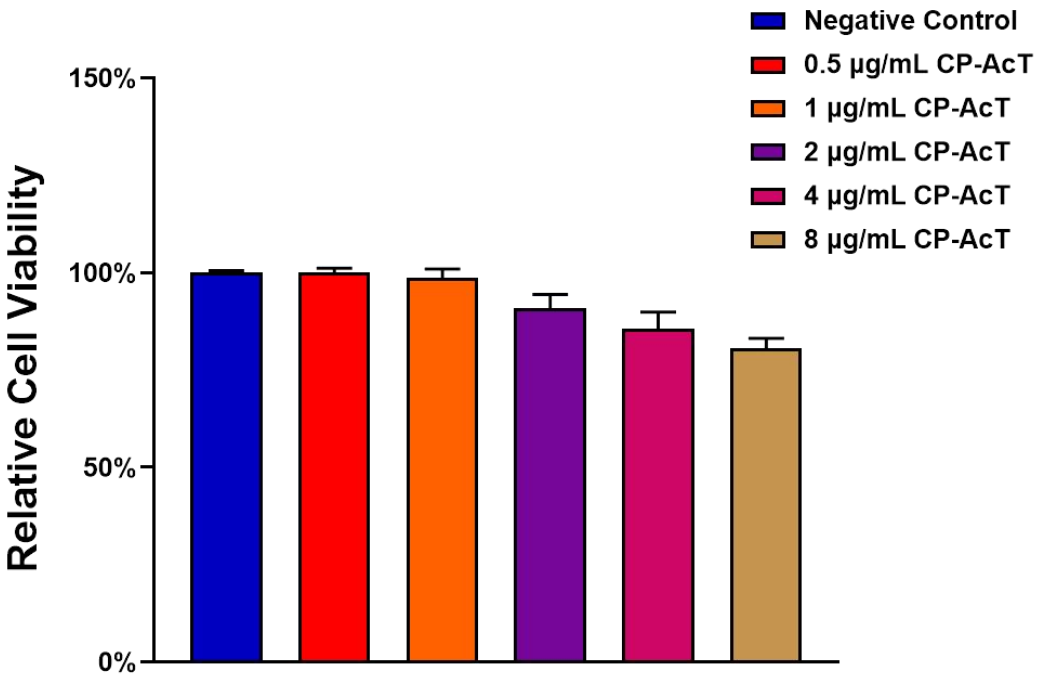

Figure 1. Effect of CP-AcT on the survival rate of A375 cell.

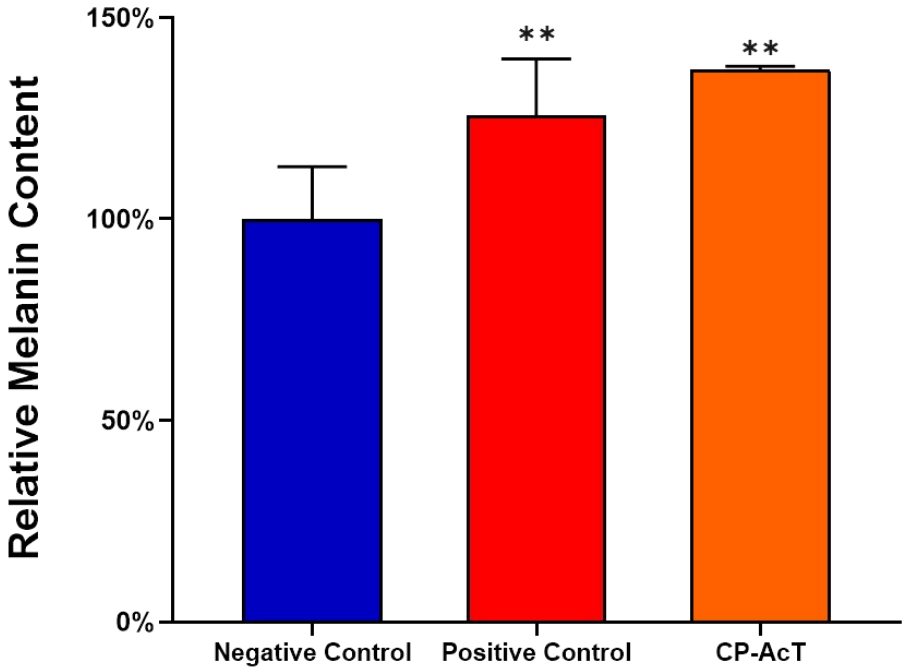

Figure 2. Effect of CP-AcT on the melanin contents of A375 cells.

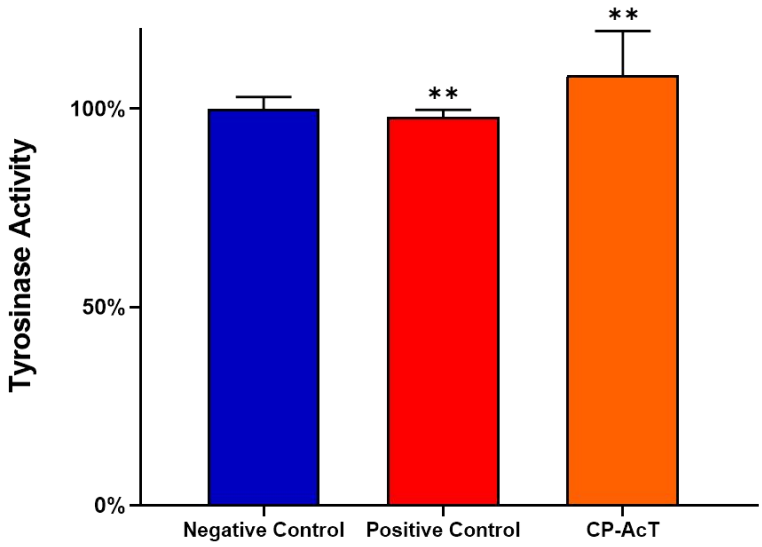

Figure 3. Effects of CP-AcT on tyrosinase activity.

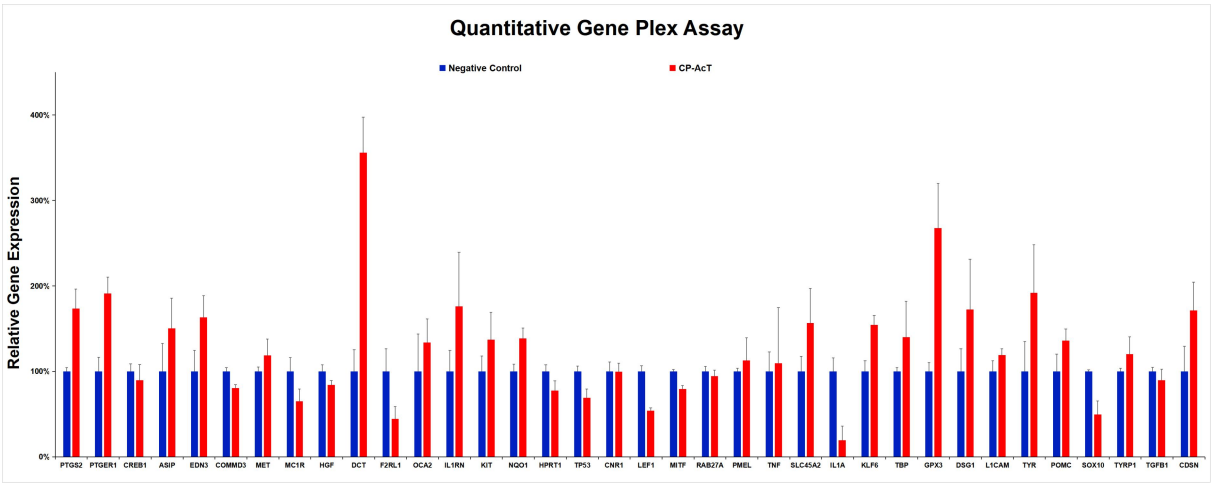

Figure 4. The result graph of the effects of CP-AcT on gene transcription.

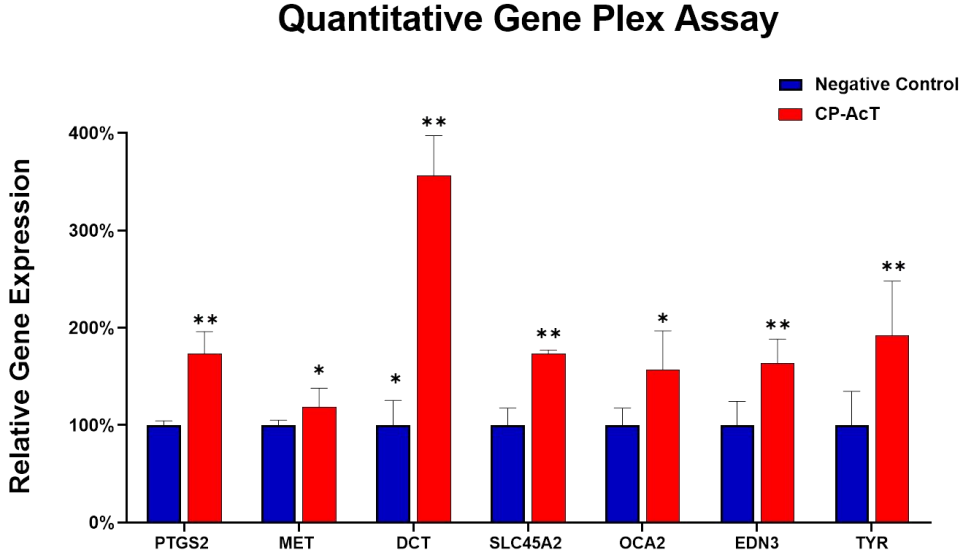

Figure 5. Analysis chart of the effects of CP-AcT on gene transcription.

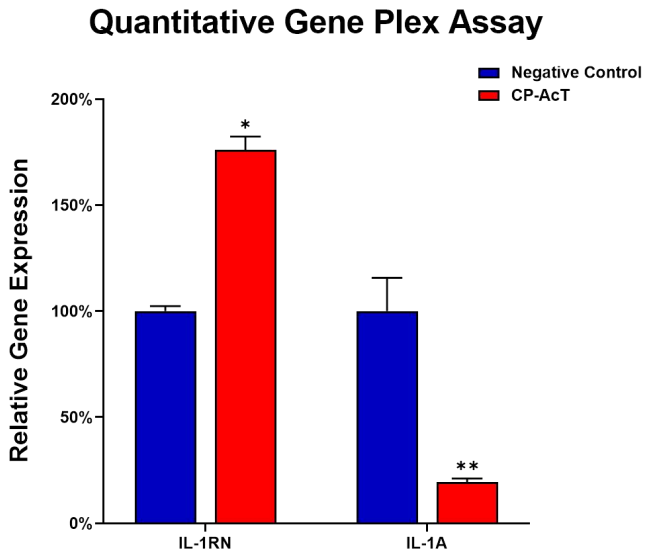

Figure 6. Analysis chart of the effects of CP-AcT on the transcription of inflammatory genes.

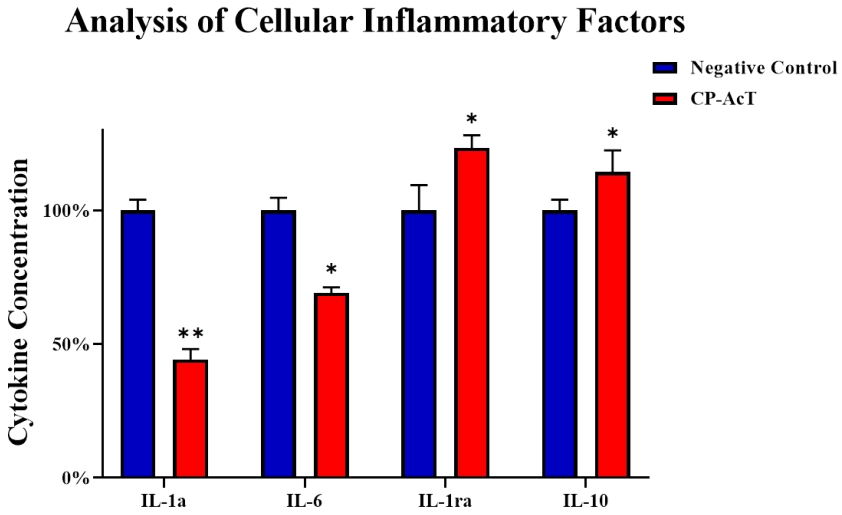

Figure 7. Analysis graph of the influence of CP-AcT on inflammatory factors.

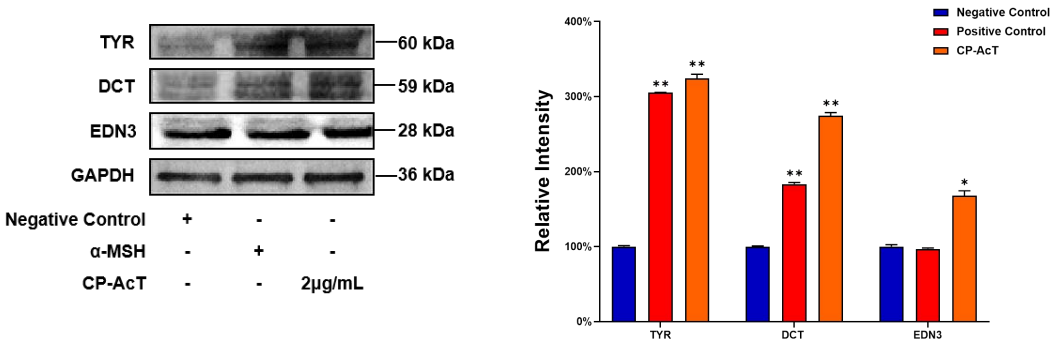

(**a**) (**b**)

Figure 8. Validation of Protein Expression in the Melanogenesis Pathway by Western Blotting: (a) Protein bands of TYR, DCT, and EDN3; (b) Quantitative analysis results of the relative intensities of the protein bands for TYR, DCT, and EDN3.

4. Discussion

This study is the first to elucidate the molecular basis by which the CP-AcT compound formulation promotes melanin synthesis through a tripartite mechanism involving "gene regulation-enzyme activity modulation-inflammatory microenvironment modulation." Our experimental results demonstrate that CP-AcT significantly upregulates the gene expression of *TYR*, *DCT*, and *EDN3* (with increases of 91.95%, 256%, and 63.28%, respectively) and validates the concurrent elevation of their protein levels via Western blot analysis. This effect may be associated with the activation of MITF, a central regulator of melanogenesis that is modulated by the cAMP/PKA and MAPK signaling pathways. Notably, the upregulation of *EDN3* expression suggests that CP-AcT may promote melanocyte proliferation and differentiation through the EDN3/EDNRB signaling axis, a mechanism complementary to the α-MSH-dependent MC1R pathway. This duality explains why CP-AcT exhibits superior melanogenic efficacy compared to α-MSH alone.

At the enzymatic activity level, CP-AcT enhances tyrosinase activity to 1.8-fold that of the control group, likely attributable to the following mechanisms: (1) The Cu^{2+} in palmitoyl copper peptide acts as a cofactor for TYR, stabilizing its binuclear copper cluster structure; (2) Acetyltyrosine enhances enzymatic reaction efficiency by reducing the substrate Km value (0.22 mM vs. 0.38 mM). Furthermore, CP-AcT's bidirectional modulation of inflammatory cytokines (80.47% downregulation of IL-1α and 76.08% upregulation of IL-1RN) holds significant implications. Chronic inflammatory microenvironments are known to suppress MITF expression via the NF-κB pathway, whereas CP-AcT may disrupt the vicious cycle of inflammation-induced hypopigmentation by inhibiting pro-inflammatory cytokines (IL-1α, IL-6) and promoting anti-inflammatory cytokines (IL-10, IL-1RN). This dual action provides novel therapeutic insights for inflammatory pigmentary disorders such as vitiligo.

Compared to existing melanogenic agents, CP-AcT offers distinct advantages: (1) its combination of natural ingredients ensures high safety, circumventing the hepatotoxicity risks associated with chemical melanogens; (2) its multi-targeted approach reduces the likelihood of drug resistance; and (3) its dual melanogenic and anti-inflammatory functions make it suitable for complex pathological contexts. However, this study has limitations: the transdermal efficacy of CP-AcT was not validated in three-dimensional skin models or animal systems, and the upstream regulatory mechanisms of EDN3 remain incompletely elucidated. Future research could integrate single-cell sequencing technologies to dissect the impact of CP-AcT on melanocyte heterogeneity and explore its clinical translational potential.

5. Conclusion

This study, through in vitro experiments, confirmed that the CP-AcT compound significantly promotes melanin synthesis in A375 cells by upregulating the expression of *TYR*, *DCT*, and *EDN3* and enhancing tyrosinase activity. Concurrently, CP-AcT effectively inhibits the expression of pro-inflammatory factors IL-1α and IL-6 while promoting the expression of anti-inflammatory factors IL-10 and IL-1RN, demonstrating notable anti-inflammatory effects. These findings suggest that the CP-AcT compound exerts synergistic effects through multiple mechanisms, not only effectively promoting melanin synthesis but also exhibiting marked anti-inflammatory properties, thereby opening up a new avenue for the treatment of pigmentary disorders. Future research will further explore the clinical translation potential of CP-AcT and its application prospects in complex pathological settings.

References

[1] D'Mello S A, Finlay G J, Baguley B C, Askarian-Amiri M E. Signaling Pathways in Melanogenesis [J]. Int J Mol Sci. 2016;17.

[2] Marks M S, Seabra M C. The melanosome: membrane dynamics in black and white [J]. Nat Rev Mol Cell Biol. 2001;2:738-48.

[3] Passeron T, Coelho S G, Miyamura Y, Takahashi K, Hearing V J. Immunohistochemistry and in situ hybridization in the study of human skin melanocytes [J]. Exp Dermatol. 2007;16:162-70.

[4] Anderson R R, Parrish J A. The optics of human skin [J]. J Invest Dermatol. 1981;77:13-9.

[5] Flaherty K T, Hodi F S, Fisher D E. From genes to drugs: targeted strategies for melanoma [J]. Nat Rev Cancer. 2012;12:349-61.

[6] Dunn K J, Brady M, Ochsenbauer-Jambor C, et al. WNT1 and WNT3a promote expansion of melanocytes through distinct modes of action [J]. Pigment Cell Res. 2005;18:167-80.

[7] Molagoda I M N, Karunarathne W, Park S R, et al. GSK-3beta-Targeting Fisetin Promotes Melanogenesis in B16F10 Melanoma Cells and Zebrafish Larvae through beta-Catenin Activation [J]. Int J Mol Sci. 2020;21.

[8] Levy C, Khaled M, Fisher D E. MITF: master regulator of melanocyte development and melanoma oncogene [J]. Trends Mol Med. 2006;12:406-14.

[9] Shibahara S, Yasumoto K, Amae S, et al. Regulation of pigment cell-specific gene expression by MITF [J]. Pigment Cell Res. 2000;13 Suppl 8:98-102.

[10] Bellei B, Picardo M. Premature cell senescence in human skin: Dual face in chronic acquired pigmentary disorders [J]. Ageing Res Rev. 2020;57:100981.

[11] Sun X, Wang T, Huang B, Ruan G, Xu A. MuicroRNA- 421 participates in vitiligo development through regulating human melanocyte survival by targeting receptor- interacting serine/threonine kinase 1 [J]. Mol Med Rep. 2020;21:858-66.

[12] Ye Q, Wen Y, Al-Kuwari N, Chen X. Association Between Parkinson's Disease and Melanoma: Putting the Pieces Together [J]. Front Aging Neurosci. 2020;12:60.

[13] Doi T, Fujiwara Y, Maruyama H. [Method for Quantitative Evaluation of the Substantia Nigra Using Phase-sensitive Inversion Recovery in 1.5 T Magnetic Resonance Imaging] [J]. Nihon Hoshasen Gijutsu Gakkai Zasshi. 2020;76:563-71.

[14] Reali M, Gouda A, Bellemare J, et al. Electronic Transport in the Biopigment Sepia Melanin [J]. ACS Appl Bio Mater. 2020;3:5244-52.